Development of Methods to Verify the Predictions of the KdV Soliton Equation

S. Ellershaw (and J. Wiseman)
L3 Laboratory Skills and Electronics, Room 228, Thursday
Submitted: November 13, 2019, Date of Experiment: 7/2/19 - 14/3/19

This work set out to verify relationship between the speed and amplitude of a soliton wave as predicted by the KdV equation. The initial experiential protocol required the manual identification of the wave peak's position in a number of video frames to allow the determination of the height and speed of the wave. Of the valid data sets collected an average χ^2 value of 0.28 was found between the recorded data and the KdV speed equation. Large percentage errors in the wave speed values, resultant from the manual methodology used, of up to 17% were found to be responsible for the low χ^2 value. In response to this an improved methodology was implemented utilising computational image processing techniques. This was found to lower the error of the wave speed values by an order of magnitude. Further work is required to determine if this improved precision would be significant enough to increase the value of $\chi^2 \approx 1$ and hence verify the speed amplitude relationship.

I. INTRODUCTION

The soliton phenomena was first recorded by John Scott Russell in his paper 'Report on waves'. He reported observing the formation of a thirty foot long and foot high wave from the bow of a barge which then travelled down the canal 'without change of form or diminution of speed'. Russell then investigated the properties of solitons further in a 30 foot wave tank constructed in his back garden [1].

The non-dispersive nature of solitons is of particular interest in modern fibre optic technology. Use of this property has the potential to increase the distance light pulses can travel between repeaters and hence increase the speed of data transfer[2].

A quantitative description of this phenomena was developed at the end of the 19th century by Korteveg and de Vries. They assumed that the liquid in question is homogeneous, incompressible and has zero viscosity and subject to the vertical gravitational force, g, and the constant atmospheric pressure acting on its free surface. Korteveg and de Vries showed that under these assumptions the propagation of a soliton wave can be described by a non-linear partial differential equation known as the KdV equation [3],

$$\frac{\partial \eta}{\partial t} + c_0 \frac{\partial \eta}{\partial x} + \Big(\frac{3c_0}{2h}\Big)\eta \frac{\partial \eta}{\partial x} + \Big(\frac{c_0 h^2}{6}\Big)\frac{\partial \eta^3}{\partial^3 x} = 0. \quad (1)$$

Where η is the vertical displacement, from equilibrium, of a liquid particle on the free surface. This can be described as a function of the particle's horizontal position, x, at time, t. h represents the water depth and c_0 is a constant given by,

$$c_0 = \sqrt{gh}. \quad (2)$$

The 3rd and 4th terms of the KdV equation describe the non-linear and dispersive nature of a soliton wave respectively. When these terms balance a stable wave is formed with a profile of the form,

$$\eta(x,t) = \eta_0 sech^2\Big(\frac{x-ct}{L}\Big). \quad (3)$$

Where η_0 is the maximum amplitude of the wave, L the characteristic length of the wave given by,

$$L = \sqrt{\frac{4h^3}{3\eta_0}}, \quad (4)$$

and c the speed of the wave given by,

$$c = \sqrt{gh}\Big(1 + \frac{\eta_0}{2h}\Big). \quad (5)$$

These relationships only hold if the wave's amplitude, wavelength and the water depth, shown in Fig.1, satisfy specific criteria. Firstly the wave amplitude must be small relative to the water depth. This is quantified by the parameter ϵ_1 given by,

$$\epsilon_1 = \frac{\eta_0}{h} \ll 1. \quad (6)$$

Secondly the wave must have a large wavelength, l, relative to the tank depth. This is similarly quantified by the parameter ϵ_2 defined as,

$$\epsilon_2 = \Big(\frac{h}{l}\Big)^2 \ll 1. \quad (7)$$

Finally, ϵ_1 and ϵ_2 must be approximately equal. This can be quantified by defining a parameter named 'Ursell number', U, which must be of order one [4],

$$U = \frac{\epsilon_1}{\epsilon_2} = \frac{\eta_0 l^2}{h^3} = O(1). \quad (8)$$

The relationship shown in Eqn.5 gives a linear equation with easily measurable parameters and hence provides an experimentally testable prediction of the KdV equation. This equation will therefore be the focus of this study. Furthermore Eqn.3 and Eqn.8 both give quantitative methods for classifying a wave as a soliton either through chi-squared analysis or the calculation of U. Both of these methods will be used and their utility compared.

A further important contribution was made by Gardner et al in 1967. They showed for a wave with a sufficiently localised shape of a non-negative initial volume the wave can evolve into the analytical soliton solution shown in Eqn.3. More specifically depending on the initial wave volume and water depth a predictable number of solitons in a chain will be produced along with a dispersive tail [5].

For the purposes of this study, the work of Gardner gives a reproducible method to form soliton waves through the use of a sluice gate to produce a square wave in a tank. This will then evolve into a chain of soliton waves as it propagates along the tank.

II. METHODS

The experimental apparatus used to to verify Eqn.5 is shown in Fig.1. The tank used was had a width of 0.15 m, a height of 0.31 m and a length of 3.10 m including a 0.28 m long sluice tank.

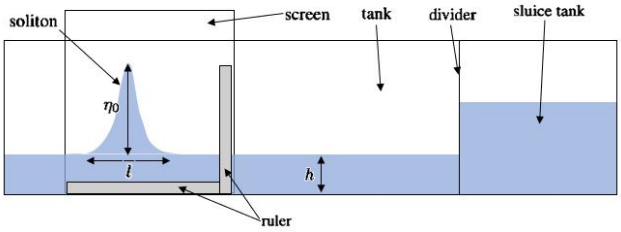

FIG. 1: A figure showing the experimental setup used and the parameters η_0, l and h. The diagram is not to scale and and the video camera which was placed opposite the screen is not shown. Please note only the primary soliton wave in the chain is shown.

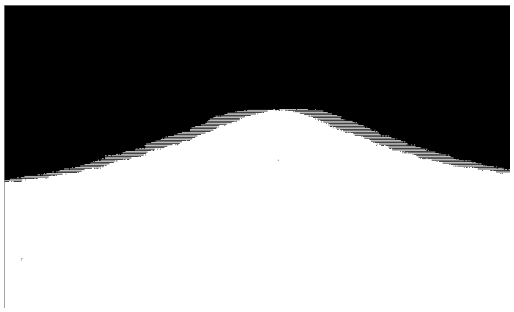

FIG. 2: Output from the binary filter used. Of note are the horizontal artefacts caused by interlacing.

Differing η_0 values were produced by filling the sluice tank to different initial water depths. The divider was then removed and the resultant wave was captured by a video camera, placed at the end of the tank to maximise the distance for the soliton chain to form. A screen was placed behind the tank to provide a plain background and maximise the contrast between the water and the surroundings. Food colouring was added to the water to further increase the contrast. The video camera was connected to a laptop and using a python script the video frames were timestamped and saved for a given time period.

Initially the video frames were manually analysed by finding the (x,y) pixel co-ordinates in each frame. η_0 was then found from the average difference between the peak and undisturbed y value in all frames. The wavelength was found in a similar manner but in relation to the x co-ordinate and then doubled. The wave speed was found from the difference in x positions of the wave peak between two adjacent video frames and then divided by the time step between the two frames. All pixel differences were then converted to metres by multiplying by the pixel to metre ratio, R_{pm}, in either the vertical or horizontal direction. R_{pm} was calculated from appropriately positioned rulers of a known length. This method was repeated for 3 values of h, which was measured using a ruler. Using Eqn.5 and Eqn.8 plots of wave speed and Ursell numbers against amplitude for differing tank depths were produced.

The method then evolved to an automated procedure using image processing techniques. Firstly, the blue channel of the input images was isolated, as blue food colouring was used. Each pixel was then put through a binary filter in which pixel values below a threshold, set arbitrarily to 100 through trial and error, were set to 0 and all others to 1. The output of this filter can be seen in Fig.2. The pixel values were then added vertically to give the y co-ordinate of the wave boundary at each x pixel, known as the wave profile.

χ^2 minimisation was then performed fitting the following equation to each wave profile,

$$y = A sech^2\Big(\frac{x-p}{d}\Big) + v. \tag{9}$$

Equating Eqn.3 and Eqn.9, it can be seen $A = \eta_0$ and $d = L$. v is the vertical shift of the function equivalent to the depth of the tank and p gives the phase shift of the function or the x pixel co-ordinate of the peak of the wave. The speed of the wave was determined, using a similar technique to the manual method, by comparing p values and the time step between adjacent video frames. The output parameters for each data set were then averaged and their standard error found. This gave the same output parameters as the manual method but additionally the χ^2 value calculated by the minimisation gave another method of soliton classification.

III. RESULTS

A plot of wave speed against amplitude, for the 3 tank depths tested, is shown in Fig.3 . The reduced-chi squared, χ^2_v, for tank depths of 5, 9 and 13 cm were calculated to be 4.3, 0.18 and 0.38 respectively. The theoretical fits are plots of Eqn.5 using the literature value of g and the experimentally measured tank depth.

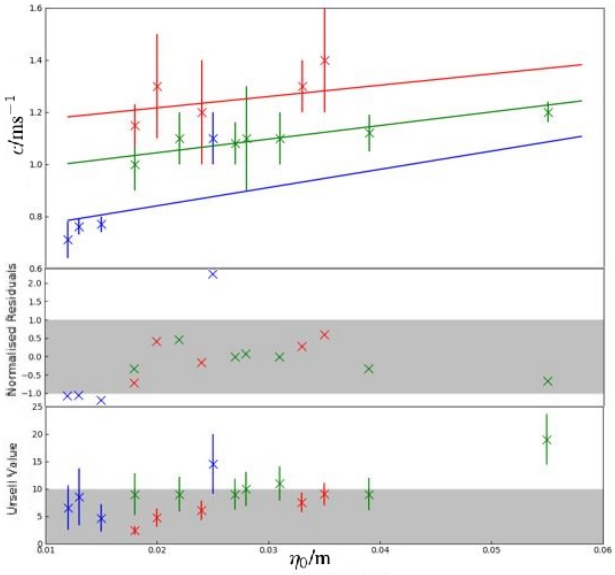

FIG. 3: A graph showing wave speed against amplitude for 3 different tank depths. Blue, (5±0.07)cm; Green, (9±0.07)cm and Red (13±0.07)cm. Error bars and theoretical fits for each tank depth are also plotted. Beneath normalised residuals and Ursell numbers are shown. The grey boxes visualise the acceptable range of values for these parameters, $O(1)$ and $\pm\sigma$ respectively.

The wave profiles produced by the computerised image processing protocol are shown in Fig.4. The χ^2 minimised fits visually show good agreement with the experiential data. χ^2_v values of 1.00, 0.75, 0.43, and 0.41, for the 0, 80, 120 and 160 ms time steps respectively, demonstrates this quantitatively.

Furthermore, as previously discussed the χ^2 minimisation process allows the determination of the parameters, and their errors, present in Eqn.3. The results of this method are

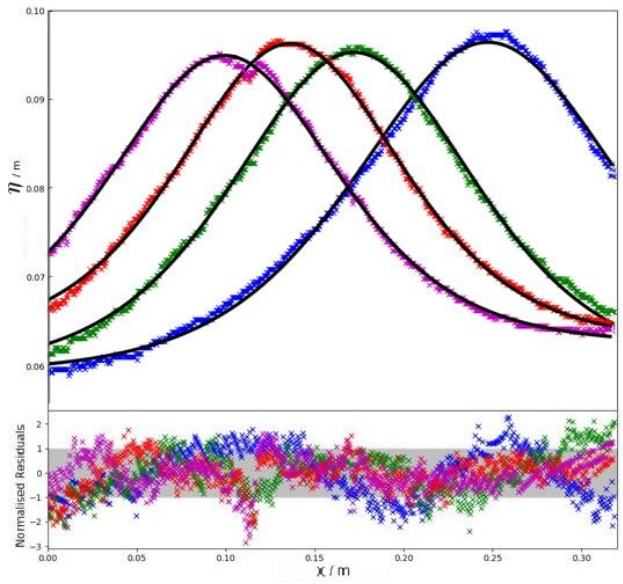

FIG. 4: A graph showing the wave profile of a soliton propagating from right to left, generated using image processing techniques. The wave is shown at 4 different times steps: Blue, 0ms; Green, 80ms; Red, 120ms and Purple, 160ms. χ^2 minimised fits of Eqn.3 for each time step are shown in black and normalised residuals of these fits are shown below. The grey box shows data points within one standard error of their trend line.

compared to values found for the same data set using the initial manual method in Table I. Notably the error in the measurement of c is reduced by an order of magnitude using the computational method.

Method	η_0 / m	c / ms^{-1}	h / m
Manual	0.038 ± 0.001	0.96 ± 0.02	0.058 ± 0.0007
Computational	0.035 ± 0.001	0.941 ± 0.005	0.0608 ± 0.008

TABLE I: A table showing a comparison between computational and manual determination of the values and errors of the key parameters, η_0, c and h

An additional wave data set was also analysed using this computational technique. The initial height in the sluice gate was made ≈12 cm which was known from previous experimentation to not form a soliton train in the tank length available. When analysed the χ_v^2 value found through the minimisation process was 170.

IV. DISCUSSION

A number of challenges were encountered when using the manual methodology to verify Eqn.5. The first of these was encountered when using Ursell numbers the classify waves as solitons. The success of this method can be seen for the anomalous data point at 5 cm tank depth with an amplitude of 0.025 m. This point is shown to lie significantly above the theoretical fit in the normal residual plot. However, it can also be seen that the data point's Ursell number is no longer $O(1)$. Therefore this point does not meet the initial conditions required for the KdV equation and so Eqn.5 can no longer be applied.

However, the anomalous 5 cm tank depth reading did not have the largest Ursell number. For the largest wave amplitude observed, 0.055 m, an Ursell number of 19.5 was recorded. This data point lies within $\pm\sigma$ of the theoretical fit though. This point is an experimental exemplification of the issues faced in the determination of a wave's Ursell number.

The horizontal distance the camera was placed away from the tank was influenced by two competing factors. On the one hand, the further away the camera was placed the greater the proportion of the wave was captured in a single frame. On the other, the closer the camera was placed to the tank the greater the pixel to metre ratio became and so the more precise the distance measurements became, see Error Appendix. Furthermore, it was decided that movement of the camera between measurements should be minimised to reduce the variability in camera angle. These factors converged to mean for large wavelengths, which corresponded to large amplitudes, the whole wave was not visible in a single frame. Therefore, it was decided to determine L a half wavelength would be measured. However, as the symmetry of the wave was no longer visible the determination of the wavelength became a more subjective measure leading to extraneous U values such as that for the 0.55 m amplitude wave.

Further critic of Fig.3 shows additional flaws in the initial experimental method used. The 5 cm tank depth contains only 4 values due to Ursell number criteria being broken for small wave amplitudes and the low level of control over wave amplitude granted by this experiential set-up. Discarding the previously discussed anomalous data point from this data set leaves only 3 points. This makes robust data analysis of this data set no longer possible.

The chi-squared analysis of the 9 and 13 cm tank depth data sets are highly informative though, with an average χ_v^2 value of 0.28. This does not allow for a positive verification of Eqn.5 as $\chi_v^2 < 1$ [6]. This small χ_v^2 value is due to the large percentage errors in the speed values recorded of up to 17%, these can be seen visually in Fig.3.

There are two main possibilities for these large errors. Firstly, when generated the wave takes a finite distance to reach an equilibrium state in which the steepening term of the KdV equation and dispersion effect are balanced. If measured before this distance the wave speed will be unstable and hence a large variance and error in the speed will be recorded. The simple solution to this issue would be to use a longer tank, such as those used in previous soliton studies [4]. However, by visual inspection of the video frames the $sech^2(x)$ shape described by Eqn.3 was clearly present suggesting the wave was fully formed. Furthermore their was no option with the equipment available to extend the tank. It was decided to instead investigate the second possibility that the experimental method used to determine the speed of each wave was flawed. The main critic of the protocol used was that the determination of the wave peak co-ordinates was a subjective decision taken by the experimentalist. A variance in these decisions between data points could therefore explain the large errors recorded.

The development of the automated image processing protocol was in direct response to the flaws in the initial method when determining Ursell numbers and the large wave speed error. The updated protocol allowed the determination of χ_v^2 for the fit of Eqn.3 to the wave profile, shown graphically in Fig.4. Therefore fitting resulting in $\chi_v^2 \approx 1$ was

used to classify a wave as a soliton. The results section shows the successful application of this approach distinguishing between already known soliton and non-soliton waves. The χ_v^2 value is also highly reproducible and has little dependency on experimentalist opinion unlike the previous method.

The automated determination of variables by the updated protocol allowed a new method for the determination of the wave speed. Table I compares the results from the two methods. For wave speed the values were found agree to within $\pm 1\sigma$, however the computational method had an order of magnitude greater precision. This increased precision is the solution that was searched for in response to the low χ_v^2 values obtained from Fig.3.

Analysing the results shown in Table I further shows that there was no significant difference in the value or the error found in η_0 between the two methods. Therefore as the computational method was less time consuming using this method preferentially in future experiments is advisable. However, there was a significant difference between the values found for h. This is offset is thought to be due to the cropping procedure that was used to edit the video frames before computational analysis. The principle was to crop to the bottom of the tank to allow the determination of h as the vertical displacement of the $sech^2(x)$ function. Unfortunately, the tank used had an opaque black border surrounding the bottom edge. Therefore the determination of the bottom of the tank in each frame was subjectively determined. It is thought that this has lead to the discrepancy shown in Table I. As the manual determination of h is a simple ruler reading which in fact leads to a higher precision this manual step should remain in future experiments.

Problems with this improved computational method still remain though. Firstly, the output video frames are interlaced, a technique designed to increase the apparent frame rate of a video without increasing the bandwidth required to transmit the picture [7]. This however leads to horizontal artefacts when video frames are analysed individually, as shown in Fig.2. In the initial manual methodology these horizontal artefacts were not an issue as only the vertical peak height was recorded. However, with the updated technique as all pixels are analysed in the production of the wave profile and so interlacing produces noise that directly affects the output values, especially χ_v^2. There are techniques which with additional time and research could be implemented to remove or lessen this affect and so potentially further improve this method.

Secondly, the problematic balance between viewing the entire wave and the precision of the distance measurements whilst ensuring the angle of the camera is maintained was not solved by the updated method. In fact the issue became of greater importance as for the χ^2 fit to be effective over half the wave is required to be in frame. No entirely satisfactory solution was found. A possibility would be to fit the camera to a track perpendicular to the tank. This would allow the camera to be repositioned for larger waves whilst ensuring the camera height and angle were maintained. This would still result in a loss of precision for larger waves which may have to be accepted as known flaw of this experimental method.

It is predicted that using this updated technique would greatly reduce the errors seen in Fig.3. However, in the initial data collection a vertical ruler was placed centrally, as shown in Fig.1. It is now realised the depth of the tank can be used as the vertical reference instead. Due to this ruler the previously recorded data could not be run through the image processing algorithm and unfortunately time did not allow for a complete re-run of the data collection stage. Therefore, in future a repeat of this work could be carried out to find if the improvements in methodology identified in this study are sufficient to verify Eqn.5.

V. CONCLUSIONS

In conclusion, an initial attempt was made to verify the relationship between the speed and amplitude of a soliton wave as predicted by the KdV equation, see Eqn.5. The initial methodology used was found to be flawed as it relied on a subjective determination of the position of the wave peak. This led to a large variance in wave speeds between readings, resulting in the percentage error of the wave speed having a value of up to 17%. Therefore, when the fit between the theoretical and recorded data was tested using χ_v^2 an average value of 0.28 was found for data sets of a size large enough to be robustly analysed. Furthermore, the determination of Ursell numbers was found to be flawed for similar reasons of subjectivity.

These initial findings lead to the development an improved computational methodology utilising image processing techniques. This allowed the determination of η and c in a more efficient and precise manner. Crucially the improved method found the standard error of c values to one order of magnitude smaller. The initial placement of the camera remains an issue in the methodology but a suggestion of using a camera track was put forward. Further experimentation is required to ascertain if the improvements in precision due to the improved methodology would result in a $\chi_v^2 \approx 1$ and hence validate Eqn.5.

References

[1] John Scott-Russell. Report on waves. In Report of the fourteenth meeting of the British Association for the Advancement of Science, volume 319, 1844.

[2] Leos Bohac. The soliton transmissions in optical fibres. Information and Communication Technologies and Services, 2010.

[3] Diederik Johannes Korteweg and Gustav De Vries. Xli. on the change of form of long waves advancing in a rectangular canal, and on a new type of long stationary waves. The London, Edinburgh, and Dublin Philosophical Magazine and Journal of Science, 39(240):422–443, 1895.

[4] Alessandro Bettini, Tullio A. Minelli, and Donatella Pascoli. Solitons in undergraduate laboratory. American Journal of Physics, 51:977–984, 11 1983.

[5] Clifford S Gardner, John M Greene, Martin D Kruskal, and Robert M Miura. Method for solving the korteweg-devries equation. Physical review letters, 19(19):1095, 1967.

[6] Ifan Hughes and Thomas Hase. Measurements and their uncertainties: a practical guide to modern error analysis. Oxford University Press, 2010.

[7] Doug Graham and Morris. What is interlaced video. VideoUniversity, 2010.

VI. ERROR APPENDIX

All of the following error analysis is in line with the methods and equations set out by Hughes and Hayes in 'Measurements and their uncertainties' [6].

A. Error analysis for position measurements by pixel co-ordinates

From observation it was seen that the open surface of the water was defined by 5 pixels at the resolution of the video camera available. Therefore the measurement was taken as the central value ± 2 pixels. As outlined in the method these pixel measurements were then converted to metre distance by multiplying by the pixel to metre ratio, R_{pm}. Therefore the uncertainty on the positions measured by pixel co-ordinates, α_{pix}, is given by,

$$\alpha_{pix} = 2R_{pm}. \tag{10}$$

This was the uncertainty in the raw data used in χ^2 minimisation in the improved methodology. The manual measurement of η_0 and l required finding the difference between two points and so the error in these parameters, $\alpha_{\eta_0,l}$, must account for the error at both pixel locations which is given by,

$$\alpha_{pix} = \sqrt{(2R_{pm})^2 + (2R_{pm})^2} = 2\sqrt{2}R_{pm} \tag{11}$$

B. Error analysis for measurement of tank depth using a ruler

The precision of the ruler used was 0.5 mm. However, similarly to the measurement of η_0 and l, the measurement of h was performed by determining the difference between two points on the ruler. Therefore the error in the manual measurement of α_{hm} is given by,

$$\alpha_{hm} = \alpha_{0.5^2+0.5^2} = 0.7mm. \tag{12}$$

C. Error analysis for averaged parameters

The values for computational determination h, c and η_0 and the manual determination of c was performed by averaging a number of results from differing video frames. Therefore the error in these averaged parameters, α_{av}, is given by,

$$\alpha_{av} = \frac{\sigma_{N-1}}{\sqrt{N}}, \tag{13}$$

where σ_{N-1} is the standard deviation values recorded for the parameter and N is the number of values recorded.

D. Error analysis for Ursell Numbers

U values were calculated using Eqn.8. Therefore the error resulting from this multi- function, α_U, is given by,

$$\alpha_U = U\sqrt{\frac{\alpha_{\eta_0}}{\eta_0} + 2\frac{\alpha_l}{l} + 3\frac{\alpha_h}{h}} \tag{14}$$